DOI: 10.1002/chem.201102287

2′-Aminoethoxy-2-amino-3-methylpyridine in Triplex-Forming Oligonucleotides: High Affinity, Selectivity and Resistance to Enzymatic Degradation

Chenguang Lou,[a] Montserrat Shelbourne,[a] Keith R. Fox,[b] and Tom Brown*[a]

Abstract: The phosphoramidite monomer of the *C*-nucleoside 2′-aminoethoxy-2-amino-3-methylpyridine (AE-MAP) has been synthesized for the first time and incorporated into triplex-forming oligonucleotides (TFOs). Ultraviolet melting and DNase I footprinting studies show that AE-MAP is a potent triplex-stabilizing monomer that is selective for GC base pairs. TFOs containing AE-MAP bind with high affinity to duplexes but only weakly to single stranded DNA. In addition, AE-MAP confers high nuclease resistance on oligonucleotides. TFOs containing AE-MAP have potential for gene knock-out and gene expression studies.

Keywords: DNA structures · nuclease resistance · nucleosides · oligonucleotides

Introduction

Triplex-forming oligonucleotides (TFOs) bind to the major groove of the DNA duplex to generate triple helices through hydrogen-bonding interactions with the exposed faces of the DNA base pairs.[1] This property renders TFOs potentially useful in inhibition of gene expression, in site-directed DNA cleavage and repair, and as tools in biotechnology.[2,3] The third strand can adopt either a parallel or antiparallel orientation relative to the target strand of the DNA duplex,[1] parallel structures being generally more stable than the antiparallel ones.[4,5] However, parallel triplexes are much more stable at low pH than at neutral pH, as protonation of cytosine ($pK_a \sim 4.5$) is necessary for the formation of C^+·GC triplets.[3,5] Many analogues have now been synthesized to overcome the pH dependency of cytosine to generate stable analogues.[6–8] The simplest strategy is to increase the basicity of N3 of cytosine to facilitate protonation at physiological pH.[6,7] This is achievable by replacing dC with a *C*-nucleoside such as 2-amino-5-(2′-deoxy-β-D-ribofuranosyl)pyridine (dAP) or 2-amino-3-methyl-5-(2′-deoxy-β-D-ribofuranosyl)pyridine (dMAP)[9–11] which are protonated at near-physiological conditions, and provide the hydrogen-bonding pattern required for triplet formation. However, despite their impressive triplex stability, the 2′-deoxyribosyl analogues of aminopyridine[9] have lower resistance to nuclease mediated degradation than their natural counterpart. This severely restricts potential in vivo applications in DNA sequence targeting and genetic therapy.

In our previous studies we showed that the 2′-methoxy analogue of dMAP (Me-MAP) produces slightly more stable triplexes than 2′-deoxycytidine (dC), while triplex stabilization by TFOs containing the bulkier 2′-methoxyethyl analogue (MOE-MAP) is very similar to dC.[12] We also found that the incorporation of Me-MAP or MOE-MAP into TFOs renders them dramatically more resistant to degradation by serum nucleases than dMAP and dC.[12] Here we report on the synthesis of a novel *C*-nucleoside 2′-*O*-aminoethyl-MAP phosphoramidite (AE-MAP) and its incorporation into oligonucleotides. The potent triplex stabilizing properties and resistance to enzyme digestion of these oligonucleotides has been demonstrated.

Results and Discussion

Synthesis of AE-MAP phosphoramidite monomer: The AE-MAP phosphoramidite monomer was synthesized from **1**[13] in seventeen steps (Scheme 1). The free OH group of **1** was alkylated in the presence of methyl bromoacetate and NaH in DMF at −5 °C to give **2** (97 %), which was then reduced with $LiBH_4$ in THF to **3** (72 %). The hydroxyl group of **3** was quantitatively displaced by phthalimide under Mitsunobu conditions to yield the protected 2′-phthalimidoethoxy derivative. Compound **4** was treated with hydrazine monohydrate in ethanol to remove the phthalimide protection (92 %) and the resultant amino function of **5** was then benzylated with benzyl bromide and NaH in DMF at 0 °C to produce tetrabenzyl-protected ribofuranoside **6** (89 % yield).

[a] C. Lou, M. Shelbourne, Prof. T. Brown
School of Chemistry
University of Southampton
Highfield, Southampton SO17 1BJ (UK)
Fax: (+44) 2380-592991
E-mail: tb2@soton.ac.uk

[b] Prof. K. R. Fox
Centre for Biological Sciences
University of Southampton
Highfield, Southampton SO17 1BJ (UK)

Supporting information for this article is available on the WWW under http://dx.doi.org/10.1002/chem.201102287.

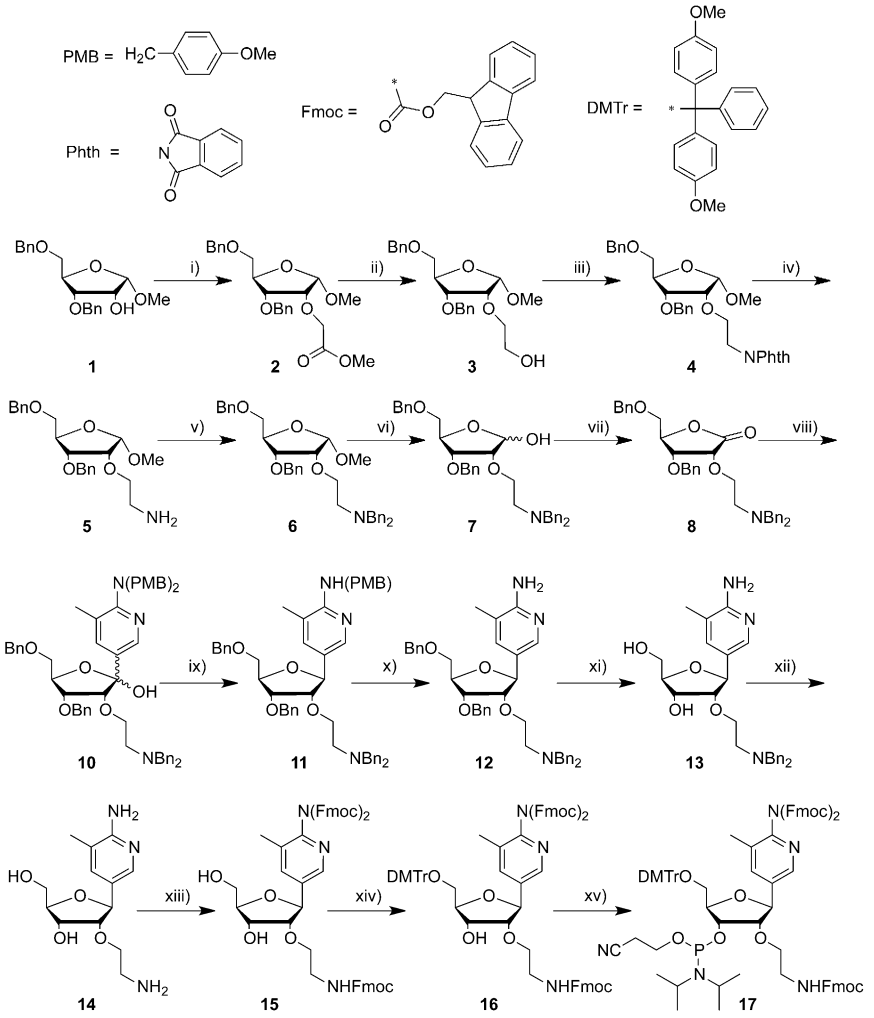

Scheme 1. i) Methyl bromoacetate, NaH, DMF, −5 °C, 5 h, 97 %; ii) $LiBH_4$, THF, RT, 1 h, 72 %; iii) phthalimide, PPh_3, DEAD, THF, RT, 1 h, 99 %; iv) $H_2NNH_2{\cdot}H_2O$, EtOH, RT, 24 h, 92 %; v) BnBr, NaH, DMF, 0 °C, 5 h, 89 %; vi) 80 % acetic acid, 1 % conc. sulfuric acid, 80 °C, 6 h, 96 %; vii) 4-methylmorpholine-*N*-oxide, tetrapropylammonium perruthenate, molecular sieves, CH_2Cl_2, RT, 5 h, 85 %; viii) **9**[12], *n*BuLi, THF, −78 °C, 8 h, 48 %; ix) triethylsilane, $BF_3{\cdot}Et_2O$, CH_2Cl_2, −78 °C, 26 h, 57 %; x) CF_3COOH, RT, 5 h, 85 %; xi) BCl_3, CH_2Cl_2, −78 °C, 7 h, 88 %; xii) Pd/C, MeOH, 50 °C, 18 h, n.a.; xiii) chlorotrimethylsilane, pyridine, RT, 2 h; Fmoc-Cl (in anhydrous MeCN), RT, 4 h; KF (in water), RT, 20 min; 63 % for four steps from **13** to **15**; xiv) DMTrCl, 8 h, RT, 78 %; xv) 2-cyanoethyl-*N*, -diisopropylchlorophosphine, DIPEA, CH_2Cl_2, 2 h, RT, 82 %.

Treatment of **6** with 80 % acetic acid and a catalytic amount of concentrated sulfuric acid gave **7**, which was oxidized to the corresponding ribolactone **8** (85 %) using tetrapropylammonium perruthenate and 4-methylmorpholine-*N*-oxide.

The subsequent three steps are identical to those for Me-MAP and MOE-MAP:[12] The resultant ribolactone was coupled with dibenzylated 2-amino-5-bromo-3-methyl-pyridine (**9**)[12] in the presence of *n*BuLi in THF to produce hemiacetal **10** as a mixture of α and β anomers, which was subsequently reduced with $Et_3SiH/BF_3{\cdot}Et_2O$ in CH_2Cl_2 to give the β-anomer of C-nucleoside **11** (57 %). The *p*-methoxybenzyl group was then cleaved in trifluoroacetic acid to provide **12** (85 %). Removal of the four benzyl groups on **12** was performed in two steps; 3′- and 5′-positions were deprotected in BF_3/CH_2Cl_2 at −78 °C to afford dibenzyl protected **13** (88 %), followed by hydrogenation with palladium on activated carbon to deprotect the remaining two benzyl groups and generate the free C-nucleoside **14**. Compound **14** was too polar to be purified by normal silica gel chromatography. Therefore, without any further purification, three in situ reactions were subsequently performed on **14**: 1) protection of the two OH groups by TMS-Cl in pyridine; 2) reaction with Fmoc-Cl to protect the two NH_2 groups; 3) deprotection of the TMS groups to liberate 3′-OH and 5′-OH to give **15** (63 % for four steps from **13** to **15**). The 5′-OH group was then selectively protected by reaction with 4′,4′-dimethoxytrityl chloride in pyridine to give **16** (78 %), which was finally converted to target monomer **17** by reaction with 2-cyanoethyl-*N*,*N*-diisopropylaminochlorophosphine under an argon atmosphere (82 %). The overall yield of the desired AE-MAP phosphoramidite monomer from compound **1** was 4.5 %.

TFO synthesis and UV triplex melting studies: Standard solid-phase phosphoramidite methods were used to synthesize the oligonucleotides containing AE-MAP. The Fmoc-protecting group not only permits AE-MAP to be incorporated into oligonucleotides using standard cycles including capping with acetic anhydride, but also allows oligonucleotide deprotection under mild conditions.[12] Pure oligonucleotides can be obtained more readily when Fmoc is chosen to protect the 2-amino group of aminopyridine than when trifluoroacetyl protection is used. This is because in the latter case the capping step with acetic anhydride has to be omitted to prevent unwanted acetylation of N2 of the aminopyridine (HPLC and CE chromatograms in the Supporting Information).

The triplex-stabilizing properties of AE-MAP were compared with Me-MAP, MOE-MAP, dMAP, 5-methyl-2′-deoxycytidine (^{Me}C), 2′-*O*-aminoethyl-5-methylcytidine (AE-^{Me}C) and dC (Figure 1).[12] The TFOs also contain 2′-aminoethoxy-T (t in Figure 1 D), an analogue of thymidine that is used in vivo to confer thermodynamic and enzymatic stability on TFOs.[14,15] The 2′-methoxyethyl analogue of S[12] (S in Figure 1 D) stabilizes CG inversions and improves sta-

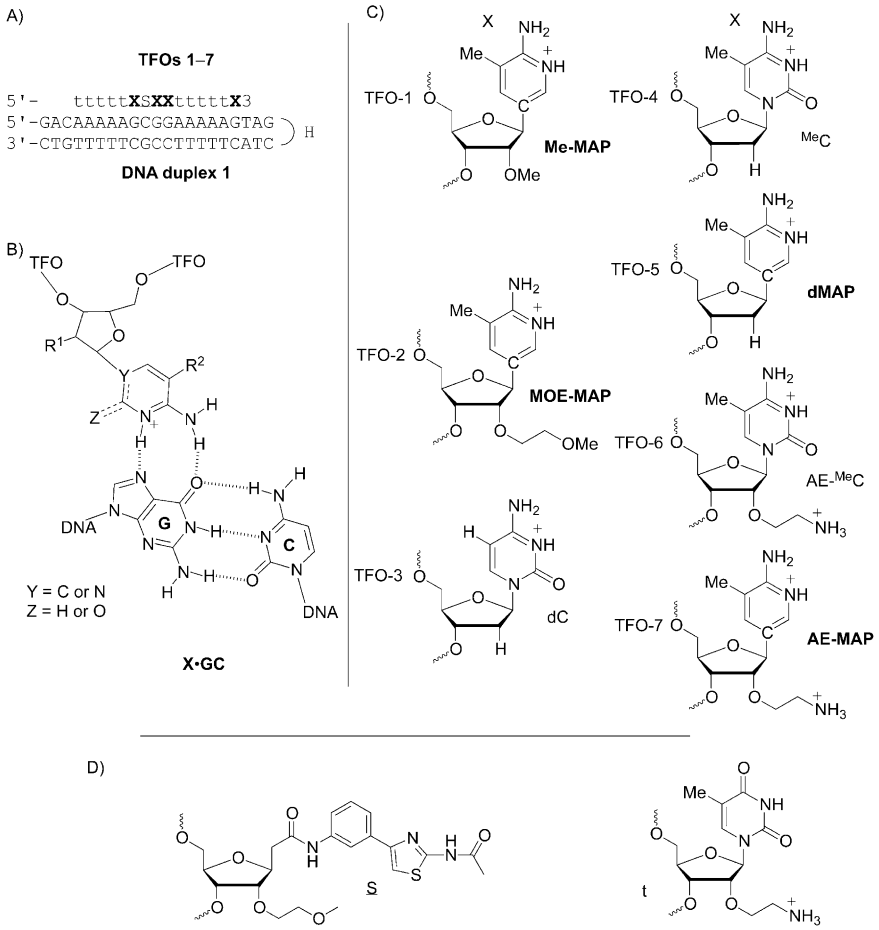

Figure 1. A) Triplexes investigated in this study. H = hexaethylene glycol linker, T = thymidine, t = 2′-aminoethoxy-T, S = 2′-methoxyethoxy-S[12]. TFO-1, X = Me-MAP. TFO-2, X = MOE-MAP. TFO-3, X = dC. TFO-4, X = ^{Me}C. TFO-5, X = dMAP. TFO-6, X = AE-^{Me}C. TFO-7, X = AE-MAP. All the TFOs are *ribo*-backbone. B) Structure of X•GC triplet. C) Modified bases (X). D) Structures of S and t in oligonucleotides.

bility to enzymatic degradation. The deoxyribose version of S was designed to recognise TA inversions in target duplexes[16,17] but it is not suitable for use in biology as it is an obvious target for DNase enzymes. The choice of TFO was dictated by the necessity for contiguous C-analogues (X in Figure 1 A) within its sequence. This ensures that AE-MAP was rigorously evaluated for its ability to bind to its target duplex even when the positively charged pyridine rings and aminoethoxy groups are clustered together. Placing X around the relatively destabilizing S further contributes to the demanding nature of the environment.

From Figure 2 and Table 1 it is clear that AE-MAP stabilizes the triple helix better than all the other analogues studied except dMAP, which is very slightly better (−0.3 °C ΔT_m/modification). The introduction of the 2′-aminoethyl group on the C-nucleoside provides higher triplex stability than 2′-methyl and 2′-methoxyethyl, which is consistent with the results on N-linked nucleosides.[8] The increased stability results from interactions between the protonated aminoethyl group and the negatively charged phosphodiester groups of the triplex.[18] Interestingly, in the N-nucleoside series the increase in T_m caused by 2′-aminoethoxy relative to 2′-methoxyethoxy substitution is only 0.8 °C per addition[19,20] whereas in the MAP *C*-nucleosides the difference is much greater (+3.7 °C per modification).

Selectivity of AE-MAP for GC over other Watson–Crick base pairs: The sequence selectivity of AE-MAP was studied on triplexes formed between TFO-7 and four target DNA duplexes that varied by a single base pair near the middle of the duplex sequence (Figure 3 and Table 2). The results show that AE-MAP binds more tightly to the desired GC base pair relative to the three incorrect ones (CG, AT and TA), consistent with the previous work on the 2′-deoxy analogue (dMAP).[10] The proximity of the promiscuous S-base probably partly neutralizes the destabilizing impact of triplet mispairing, but despite this it is clear that AE-MAP is selective for GC, at least within the context of the triplex sequence investigated in this study.

Table 1. UV-melting analysis.[a]

X	T_m	ΔT_m/modification
dMAP	60.5	+3.5
AE-MAP	59.0	+3.2
AE-^{Me}C	57.8	+2.9
^{Me}C	54.0	+1.9
Me-MAP	49.2	+0.7
dC	46.4	0
MOE-MAP	44.5	−0.5

[a] T_m values were determined in 10 mM NaH_2PO_4/Na_2HPO_4 buffer (pH 7.0) containing 200 mM NaCl. The concentration of TFO: target DNA was 3.0 μM:1.0 μM. Each value is the average of two independent experiments. The T_m values for dMAP, ^{Me}C, Me-MAP, dC and MOE-MAP are from our previous studies.[12] Calculated ΔT_m/modifications are ±0.2 °C. ΔT_m/mod indicates the increase in T_m *per* modification (4 modifications per TFO).

Selectivity of AE-MAP for DNA duplexes relative to single-stranded DNA: The interaction of TFO-7 with its antiparallel complementary purine-rich single-stranded DNA was also studied (Figures 4 and 5 and Table 3). There was a large decrease in duplex T_m (−13.5 °C) when four dC resi-

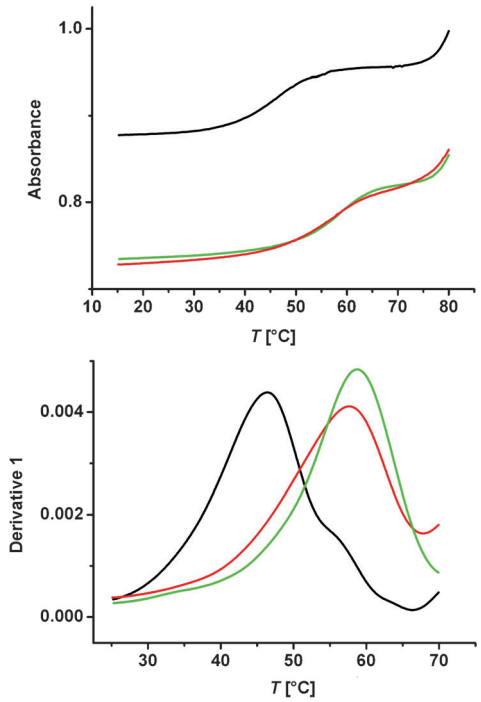

Figure 2. UV melting curves (top) and derivatives (bottom) of TFOs with target hairpin duplex 1 at pH 7.0: TFO-3, X = dC (black), TFO-6, X = AE-^{Me}C (red) and TFO-7, X = AE-MAP (green). UV melting curves were recorded at 280 nm. Triplex sequence in Figure 1 A.

Figure 3. Selectivity studies of AE-MAP (X) towards Watson–Crick base pairs (YZ): 3 = propanol, t = 2′-aminoethoxy-T, S = 2′-methoxyethoxy-S; duplex 1, YZ = GC; duplex 2, YZ = CG; duplex 3, YZ = AT; duplex 4, YZ = TA.

Table 2. Selectivity, T_m values [°C] of triplexes between TFO-7 (X = AE-MAP) and target DNA duplexes.[a]

Triplet (X·YZ)	X·GC	X·CG	X·AT	X·TA
T_m	59.0	49.8 (−9.2)	51.9 (−7.1)	54.6 (−4.4)

[a] Values in parentheses are the difference between the T_m with a GC base pair target and the T_m with the incorrect CG, AT and TA base pairs. Experiments were carried out at pH 7.0 using the same conditions as in Table 1.

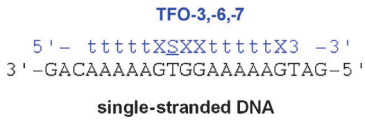

Figure 4. Affinity studies of TFO-3,-6,-7 towards antiparallel complementary single-stranded DNA: t = 2′-aminoethoxy T, S = 2′-methoxyethoxy-S. TFO-3, X = dC. TFO-6, X = AE-^{Me}C. TFO-7, X = AE-MAP.

dues were replaced by AE-MAP, which is consistent with the previous results on 2′-modified dMAP analogues.[12] In contrast, an increase in T_m of 6.1 °C was observed on replacing the four dC residues with AE-^{Me}C, indicating that the AE-^{Me}C·G base pair is more stable than CG in contrast to AE-MAP·G which is much less stable. Therefore, though both types of TFO show potent triplex stabilization, unlike AE-^{Me}C the incorporation of AE-MAP renders oligonucleotides selective for double rather than single stranded DNA. This major reduction in single strand binding (−19.6 °C for AE-MAP relative to AE-MeC) should be an advantage in triplex-mediated gene inhibition studies because single stranded DNA or RNA can potentially sequester TFOs.

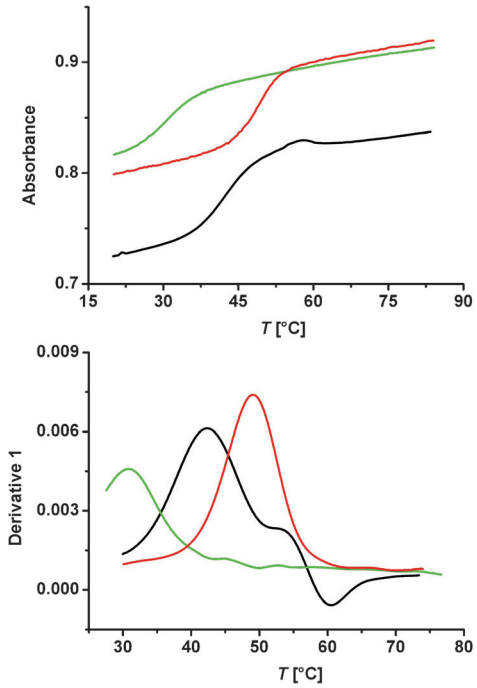

Figure 5. UV melting curves (top) and derivatives (bottom) of TFOs 3,6,7 with Watson–Crick complementary single stranded DNA: TFO-3, X = dC (black). TFO-6, X = AE-^{Me}C (red). TFO-7, X = AE-MAP (green). Duplex sequence in Figure 4. Experiments were performed in 10 mM sodium phosphate pH 7.0, 200 mM NaCl. UV melting curves were recorded at 260 nm.

Table 3. T_m values for duplex melting.[a]

TFO	Nucleoside (X)	T_m [°C]	ΔT_m (X-dC)
TFO-3	dC	43.0	–
TFO-6	AE-^{Me}C	49.1	+6.1
TFO-7	AE-MAP	30.6	−13.6

[a] T_m values are an average of three melting temperatures. The experiments were performed in 10 mM NaH_2PO_4/Na_2HPO_4 buffer pH 7.0 containing 200 mM NaCl: single stranded DNA/TFO = 1.05 μM/1.00 μM.

DNase-1 footprinting: In addition to the UV melting results, DNase I footprinting was carried out with TFO-7 to compare AE-MAP with other nucleotides in TFO-1, -3, -4, -5 and -6 (Me-MAP, dC, ^{Me}C, dMAP and AE-^{Me}C respectively). For these experiments we used a DNA fragment that contained the same target duplex as the UV melting studies.[12] DNase I footprinting experiments comparing AE-MAP with dMAP and ^{Me}C at pH 7.5 are shown in Figure 6.

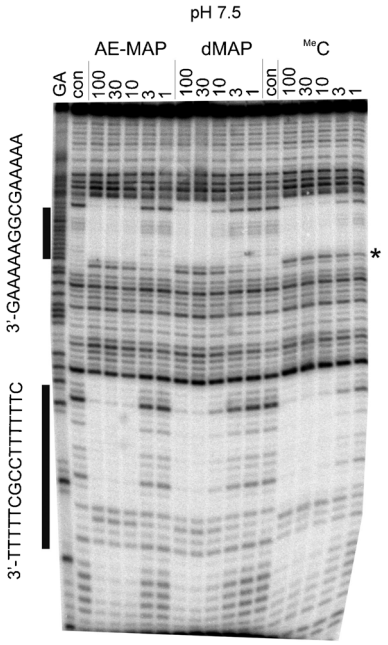

Figure 6. DNase I footprinting of TFOs containing AE-MAP (TFO-7); dMAP (TFO-5) and ^{Me}C (TFO-4). The experiment was performed in 10 mM Tris-HCl pH 7.5 containing 50 mM NaCl. TFO concentrations (nM) are shown at the top of each gel lane. Tracks labeled "Con" are control lanes in the absence of added TFO. The track labeled "GA" is a marker specific for purines. The locations of the two triplex target sites are indicated by the bars.

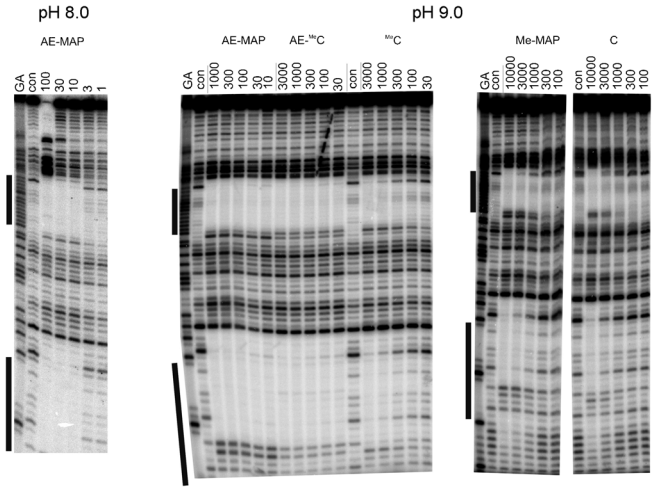

Figure 7. DNase I footprinting of TFOs containing AE-MAP (TFO-7) at pH 8.0 and AE-MAP (TFO-7), AE-^{Me}C (TFO-6), ^{Me}C (TFO-4), Me-MAP (TFO-1) and dC (TFO-3) at pH 9.0. The experiments were performed in 10 mM Tris-HCl pH 8.0 or 9.0 containing 50 mM NaCl. TFO concentrations (nM) are shown at the top of each gel lane. Tracks labeled "Con" are control lanes in the absence of added TFO. The track labeled 'GA' is a marker specific for purines. The locations of the two triplex target sites are indicated by the bars.

The DNA fragment contains two identical copies of the triplex target site (indicated by the bars), which are arranged in opposite orientations; the upper site shows the purine-containing strand of the target, while the lower site reveals the pyrimidine-containing strand. TFO-7 produces a clear footprint, which extends to concentrations below 10 nM, similar to that seen with ^{Me}C and a little stronger than with dMAP. At this pH there is little difference between these TFOs containing different C analogues as the interaction is dominated by the strong t•AT triplet (t = 2′aminoethoxy-T).

One interesting feature of these footprints is evident in the enhancements that are produced at the 3′- (lower) end of the upper (purine-containing) strand indicated by the asterisk. This effect has often been noted at triplex-duplex junctions. This enhancement is one base higher with ^{Me}C than AE-MAP, suggesting that the terminal ^{Me}C•GC triplet is fraying, while AE-MAP•GC is not. Since the triplexes are stable at pH 7.5 we extended these studies to higher pH values and the results are shown in Figure 7.

TFO-7 produces a very similar footprint at pH 8.0 to that seen at pH 7.5, extending to concentrations below 10 nM. At pH 9.0 both TFOs containing the 2′-aminoethoxy substituent (AE-MAP and AE-^{Me}C) still produced very stable complexes, while ^{Me}C, Me-MAP and dC required much higher concentrations to bind (300 nM, 1 μM and 3 μM respectively). These triplexes are all stabilized by the 2′-aminoethoxy-T•AT triplet (t•AT) and therefore occur at higher pH values than would have been the case with T•AT, but the additional enhancement resulting from the 2′-aminoethoxy group on MAP is clear, producing a footprint at concentrations that at about 300-fold lower.

The above footprinting studies indicate that AE-MAP and t constitute a potent triplex-stabilizing combination at high pH, enhancing the binding of the TFO to its target duplex. They are therefore likely to function effectively under physiological conditions where only low concentrations of TFO are likely to reach the genomic target. The importance of the 2′-aminoethoxy group in enhancing the binding of TFOs has been demonstrated previously, and the present study lends further support to these findings.[21] It also implies that triplex binding could be further enhanced if S is replaced by 2′-aminoethoxy S.[22]

Resistance to nuclease degradation: We have previously observed rapid nuclease-mediated degradation of TFOs containing dMAP in serum,[12] thus making them unsuitable for in vivo applications. It is known that the 2′-aminoethyl modification on N-linked nucleosides renders oligonucleotides strongly resistant to enzyme digestion.[14] We therefore investigated whether the same is true of 2′-aminoethoxy modified C-nucleosides by evaluating an oligonucleotide containing several AE-MAP residues (TFO-8).

The oligonucleotides used in this enzymatic degradation resistance study (Table 4) are identical in their basic sequence to those containing Me-MAP and MOE-MAP which were studied previously.[12] Oligonucleotides modified with dMAP (TFO-9) and dC (TFO-10) were compared with AE-MAP (TFO-8). TFO-8, -9 and -10 were incubated in a medium containing fetal bovine serum (FBS) for various periods from 1–24 h and their stability was determined by denature PAGE analysis (Figure 8).

Table 4. Oligonucleotides used in nuclease degradation experiments.[a]

TFO code	X	Stability
TFO-8	AE-MAP	+
TFO-9	dMAP	–
TFO-10	dC	–

[a] TFO Sequence = TXTTXTTTTTTXTTXTTXXT.

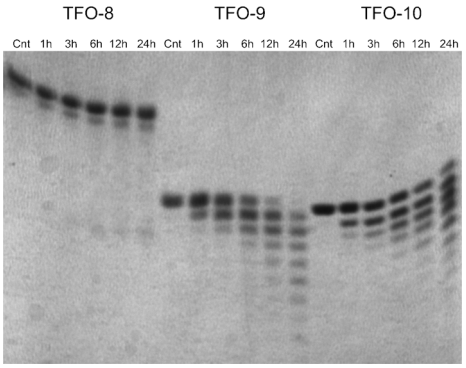

Figure 8. 20% PAGE denaturing gel showing the time-course of TFO degradation in serum, following incubation of TFO-8, -9 and -10 at pH 7.0, 37°C. Samples were incubated for 1, 3, 6, 12 and 24 h. The negative control (Cnt) was incubated at 37°C for 24 h in the absence of serum. The gel was visualized by UV shadowing.

The controls TFO-10 (dC) and TFO-9 (dMAP) were rapidly degraded, with the appearance of shorter length bands after only 1 h incubation. The dMAP-containing TFO was extensively degraded after 6 h incubation, and there was no intact TFO after 24 h. TFO-10 was slightly more resistant to degradation than TFO-9: about half of the intact TFO remained after 6 h incubation. By comparison, the TFO containing AE-MAP (TFO-8) was largely intact even after 24 h incubation though minor degradation was observed. This is probably due to the loss of the "unprotected" 3′-thymidine. No further degradation of TFO-8 was observed in our experiments probably due to the presence of the 2′-aminoethoxy group and the protonated primary amine which may inhibit both enzyme binding and phosphodiester cleavage. Clearly AE-MAP confers much more resistance towards nucleases-mediated oligonucleotide degradation than the 2′-deoxyribose analogues dMAP and dC. Interestingly dMAP is particularly susceptible to enzymatic degradation.

Conclusion

AE-MAP phosphoramidite monomer has been synthesized from 1-*O*-methyl-3,5-di-*O*-benzyl-α-D-ribofuranoside (**1**) and dibenzylated 2-amino-5-bromo-3-methyl-pyridine (**9**). UV-melting and DNase I footprinting studies on TFOs containing AE-MAP indicate that it is a potent triplex-stabilizing monomer that confers high nuclease resistance on oligonucleotides. AE-MAP binds more tightly to the desired GC base pair than CG, AT and TA and incorporation of AE-MAP into oligonucleotides suppresses duplex formation with complementary antiparallel Watson–Crick strands, in contrast to the corresponding sequences containing AE-^{Me}C. These properties suggest that TFOs containing the C-nucleoside AE-MAP have potential in site-directed gene knock-out and inhibition of gene expression.

Acknowledgements

This work was supported by a research grant from BBSRC under the SCIBS initiative. We thank ORSAS for funding a studentship to C. Lou and ATDBio for oligonucleotide synthesis.

[1] M. D. Frankkamenetskii, S. M. Mirkin, *Annu. Rev. Biochem.* **1995**, *64*, 65–95.
[2] T. Le Doan, L. Perrouault, D. Praseuth, N. Habhoub, J. L. Decout, N. T. Thuong, J. Lhomme, C. Helene, *Nucleic Acids Res.* **1987**, *15*, 7749–7760.
[3] H. E. Moser, P. B. Dervan, *Science* **1987**, *238*, 645–650.
[4] P. A. Beal, P. B. Dervan, *Science* **1991**, *251*, 1360–1363.
[5] D. M. Gowers, K. R. Fox, *Nucleic Acids Res.* **1999**, *27*, 1569–1577.
[6] M. Duca, P. Vekhoff, K. Oussedik, L. Halby, P. B. Arimondo, *Nucleic Acids Res.* **2008**, *36*, 5123–5138.
[7] K. R. Fox, *Curr. Med. Chem.* **2000**, *7*, 17–37.
[8] D. A. Rusling, V. J. Broughton-Head, T. Brown, K. R. Fox, *Curr. Chem. Biol.* **2008**, *2*, 1–10.
[9] P. J. Bates, C. A. Laughton, T. C. Jenkins, D. C. Capaldi, P. D. Roselt, C. B. Reese, S. Neidle, *Nucleic Acids Res.* **1996**, *24*, 4176–4184.
[10] S. Hildbrand, A. Blaser, S. P. Parel, C. J. Leumann, *J. Am. Chem. Soc.* **1997**, *119*, 5499–5511.
[11] S. Hildbrand, C. Leumann, *Angew. Chem.* **1996**, *108*, 2100–2102; *Angew. Chem. Int. Ed. Engl.* **1996**, *35*, 1968–1970.
[12] C. Lou, Q. Xiao, R. R. Tailor, N. Ben Gaied, N. Gale, M. E. Light, K. R. Fox, T. Brown, *Med. Chem. Commun.* **2011**, *2*, 550–558.
[13] C. G. Lou, Q. A. Xiao, L. Brennan, M. E. Light, N. Vergara-Irigaray, E. M. Atkinson, L. M. Holden-Dye, K. R. Fox, T. Brown, *Bioorg. Med. Chem.* **2010**, *18*, 6389–6397.
[14] B. Cuenoud, F. Casset, D. Husken, F. Natt, R. M. Wolf, K. H. Altmann, P. Martin, H. E. Moser, *Angew. Chem.* **1998**, *110*, 1350–1353; *Angew. Chem. Int. Ed.* **1998**, *37*, 1288–1291.
[15] A. Majumdar, N. Puri, N. McCollum, S. Richards, B. Cuenoud, P. Miller, M. M. Seidman, in *Therapeutic Oligonucleotides* **2003**, pp. 141–153.
[16] D. Guianvarc'h, R. Benhida, J. L. Fourrey, R. Maurisse, J. S. Sun, *Chem. Commun.* **2001**, 1814–1815.
[17] D. A. Rusling, V. E. C. Powers, R. T. Ranasinghe, Y. Wang, S. D. Osborne, T. Brown, K. R. Fox, *Nucleic Acids Res.* **2005**, *33*, 3025–3032.
[18] M. J. J. Blommers, F. Natt, W. Jahnke, B. Cuenoud, *Biochemistry* **1998**, *37*, 17714–17725.
[19] M. Vonpierre, *Helv. Chim. Acta* **1995**, *78*, 486–504.
[20] N. Puri, A. Majumdar, B. Cuenoud, F. Natt, P. Martin, A. Boyd, P. S. Miller, M. M. Seidman, *Biochemistry* **2002**, *41*, 7716–7724.
[21] S. Buchini, C. J. Leumann, *Angew. Chem.* **2004**, *116*, 4015–4018; *Angew. Chem. Int. Ed.* **2004**, *43*, 3925–3928.
[22] Y. Wang, D. A. Rusling, V. E. C. Powers, O. Lack, S. D. Osborne, K. R. Fox, T. Brown, *Biochemistry* **2005**, *44*, 5884–5892.

Received: July 25, 2011
Published online: November 30, 2011

